Electronic Supplementary Material (ESI) for New Journal of Chemistry.
This journal is © The Royal Society of Chemistry and the Centre National de la Recherche Scientifique 2021

Supporting information

The nitrosyl linkage photoisomerization in heteroleptic fluoride ruthenium complexes derived from labile nitrate precursors

Artem A. Mikhailov[a], Vladislav Yu. Komarov[a], Denis P. Pishchur[a], Dominik Schaniel[b] and Gennadiy A. Kostin[a]

[a] Nikolaev Institute of Inorganic Chemistry, Siberian Branch of the Russian Academy of Sciences, 3 Acad. Lavrentiev Avenue, Novosibirsk 630090, Russian Federation

[b] Universite´ de Lorraine, CNRS, CRM2, UMR 7036, Nancy 54000, France

Table S1. Experimental and refinement details.

Complex	$[RuNO(NH_3)_2(H_2O)_2F]SiF_6$	$[RuNOPy(NH_3)_2(NO_3)F]_2SiF_6{\cdot}H_2O$	$[RuNOPy(NH_3)_2(H_2O)F](ClO_4)_2$	$[(RuNOPy(NH_3)_2F)_2(\mu\text{-}O_2H_3)](ClO_4)_3$
Empirical formula	$F_7H_{10}N_3O_3RuSi$	$C_{10}H_{26}F_8N_{10}O_{10}Ru_2Si$	$C_5H_{13}Cl_2FN_4O_{10}Ru$	$C_{6.67}H_{16.67}Cl_2F_{1.33}N_{5.33}O_{10.67}Ru_{1.33}$
Formula weight	362.27	828.64	480.16	573.25
Temperature/K	150	150	150	100
Crystal system	orthorhombic	triclinic	monoclinic	monoclinic
Space group	Pnma	P-1	$P2_1/c$	$P2_1/c$
a/Å	19.2150(5)	6.7669(3)	18.3073(8)	18.6327(8)
b/Å	7.7578(3)	9.2867(4)	8.3396(3)	13.8821(5)
c/Å	6.2397(2)	11.4450(6)	10.2007(4)	10.4352(5)
α/°	90	103.780(2)	90	90
β/°	90	101.152(2)	104.729(2)	96.730(4)
γ/°	90	103.764(2)	90	90
Volume/Å^3	930.13(5)	654.19(5)	1506.22(10)	2680.6(2)
Z	4	1	4	6
ρ_{calc}g/cm^3	2.587	2.103	2.117	2.131
μ/mm^{-1}	1.924	1.323	1.465	1.526
F(000)	704.0	410.0	952.0	1704.0
Crystal size/mm^3	0.388 × 0.369 × 0.194	0.137 × 0.107 × 0.059	0.284 × 0.145 × 0.091	0.036 × 0.021 × 0.012
Radiation	MoKα (λ = 0.71073)	MoKα (λ = 0.71073)	MoKα (λ = 0.71073)	MoKα (λ = 0.71073)
2Θ range for data collection/°	4.24 to 59.318	3.8 to 61.44	4.602 to 63.002	4.402 to 65.83
Index ranges	$-24 \le h \le 26$, $-10 \le k \le 9$, $-8 \le l \le 5$	$-9 \le h \le 9$, $-13 \le k \le 13$, $-15 \le l \le 15$	$-26 \le h \le 22$, $-11 \le k \le 12$, $-14 \le l \le 13$	$-28 \le h \le 27$, $-21 \le k \le 20$, $-15 \le l \le 14$
Reflections collected	4440	12459	22377	44028
Independent reflections	1406 [R_{int} = 0.0238, R_{sigma} = 0.0248]	3865 [R_{int} = 0.0312, R_{sigma} = 0.0368]	5005 [R_{int} = 0.0513, R_{sigma} = 0.0442]	9455 [R_{int} = 0.0597, R_{sigma} = 0.0543]
Data/restraints/ parameters	1406/0/82	3865/0/193	5005/0/244	9455/1/380
Goodness-of-fit on F^2	1.262	1.056	1.123	1.071
Final R indexes [I>=2σ (I)]	R_1 = 0.0272, wR_2 = 0.0542	R_1 = 0.0238, wR_2 = 0.0442	R_1 = 0.0404, wR_2 = 0.0785	R_1 = 0.0395, wR_2 = 0.0758
Final R indexes [all data]	R_1 = 0.0284, wR_2 = 0.0546	R_1 = 0.0285, wR_2 = 0.0458	R_1 = 0.0489, wR_2 = 0.0821	R_1 = 0.0701, wR_2 = 0.0924
Largest diff. peak/hole / e Å^{-3}	0.42/-0.89	0.48/-0.66	0.61/-0.74	1.93/-1.40

The Hirshfeld surfaces were calculated using Crystal Explorer [1,2]. This program allows the normalized contact distance d_{norm} to be mapped onto the generated Hirshfeld surface. It is customary to map d_{norm} using a red–white–blue scheme, where red denotes close intermolecular contacts (negative d_{norm}), blue denotes longer contacts (positive d_{norm}) and white denotes intermolecular contacts equal to the van der Waals radii of atoms in contact (d_{norm} = 0). It is possible to obtain two-dimensional plots (fingerprint plots) from the surfaces mapped with d_{norm} values. Derived from the Hirshfeld surface, these 2D-fingerprint plots provide a visual summary of the frequency of each combination of d_e (radius of external atom) and d_i (radius of internal atom) across the surface of a molecule, so they not only indicate which intermolecular interactions are present, but also the relative area of the surface corresponding to each kind of interaction. Points on the plot with no contribution on the surface are left uncoloured, and points with a contribution to the surface are coloured blue for a small contribution through green to red for points with the greatest contribution.

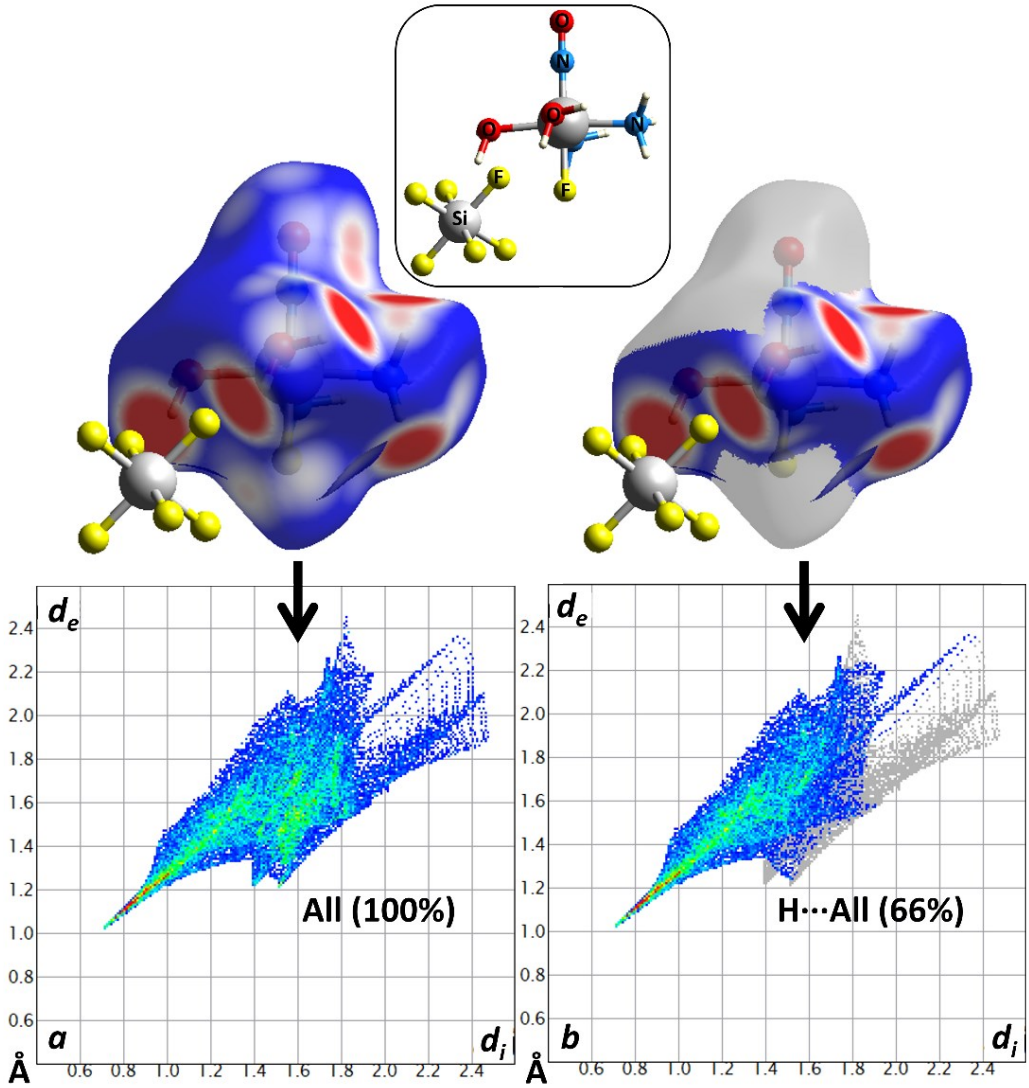

Fig. S1. The panel *a* represents the total Hirshfeld surface of the $[RuNO(NH_3)_2(H_2O)_2F]^{2+}$ cation and corresponding two-dimensional fingerprint. The panel *b* shows the surface formed by the contacts of hydrogen atoms with other surrounding atoms and corresponding 2D fingerplot.

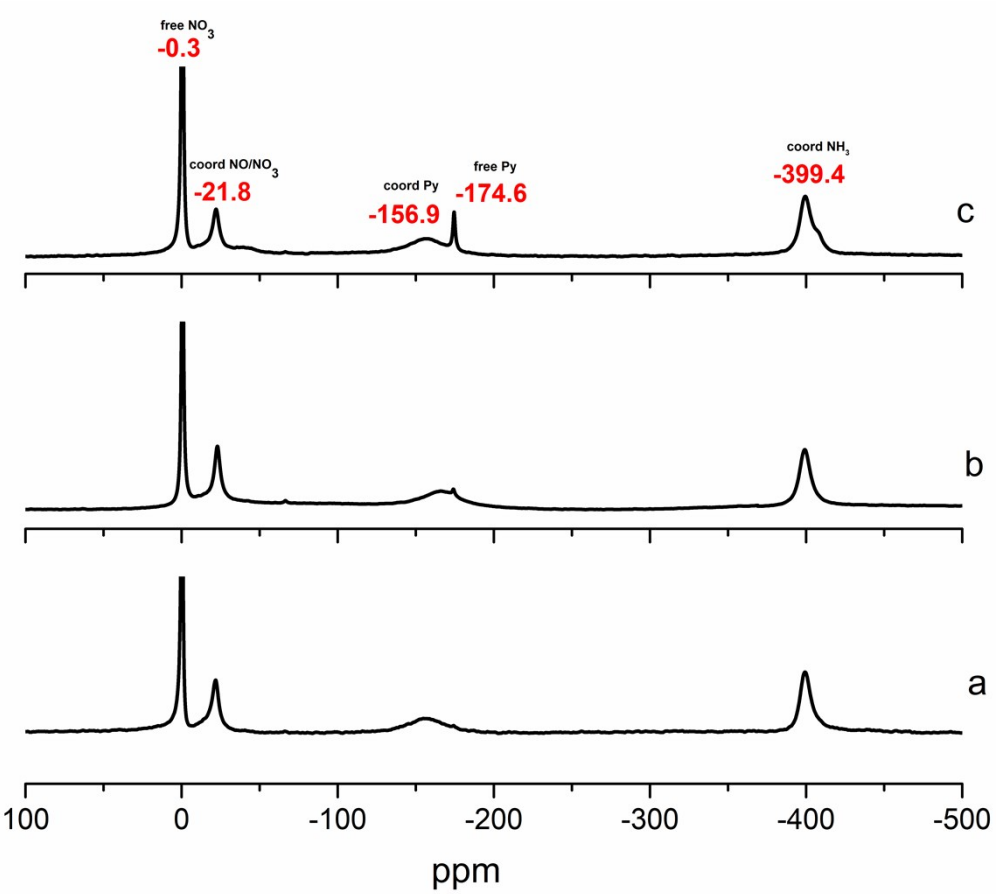

Fig. S2. ^{14}N - NMR spectra of water solution of $[RuNO(NH_3)_2(Py)_2(NO_3)](NO_3)_2$: a) immediately after preparation of the solution; b) after 10 days at room temperature; c) after heating for 4 h at 85°C.

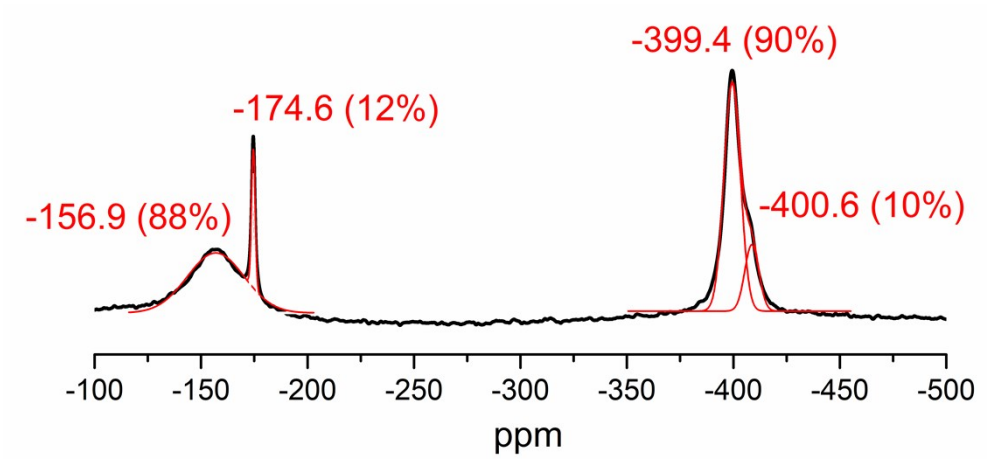

Fig. S3. The Gaussian fit of the peaks of the spectra of the $[RuNO(NH_3)_2(Py)_2(NO_3)](NO_3)_2$ after the heating (4 h, 85°C).

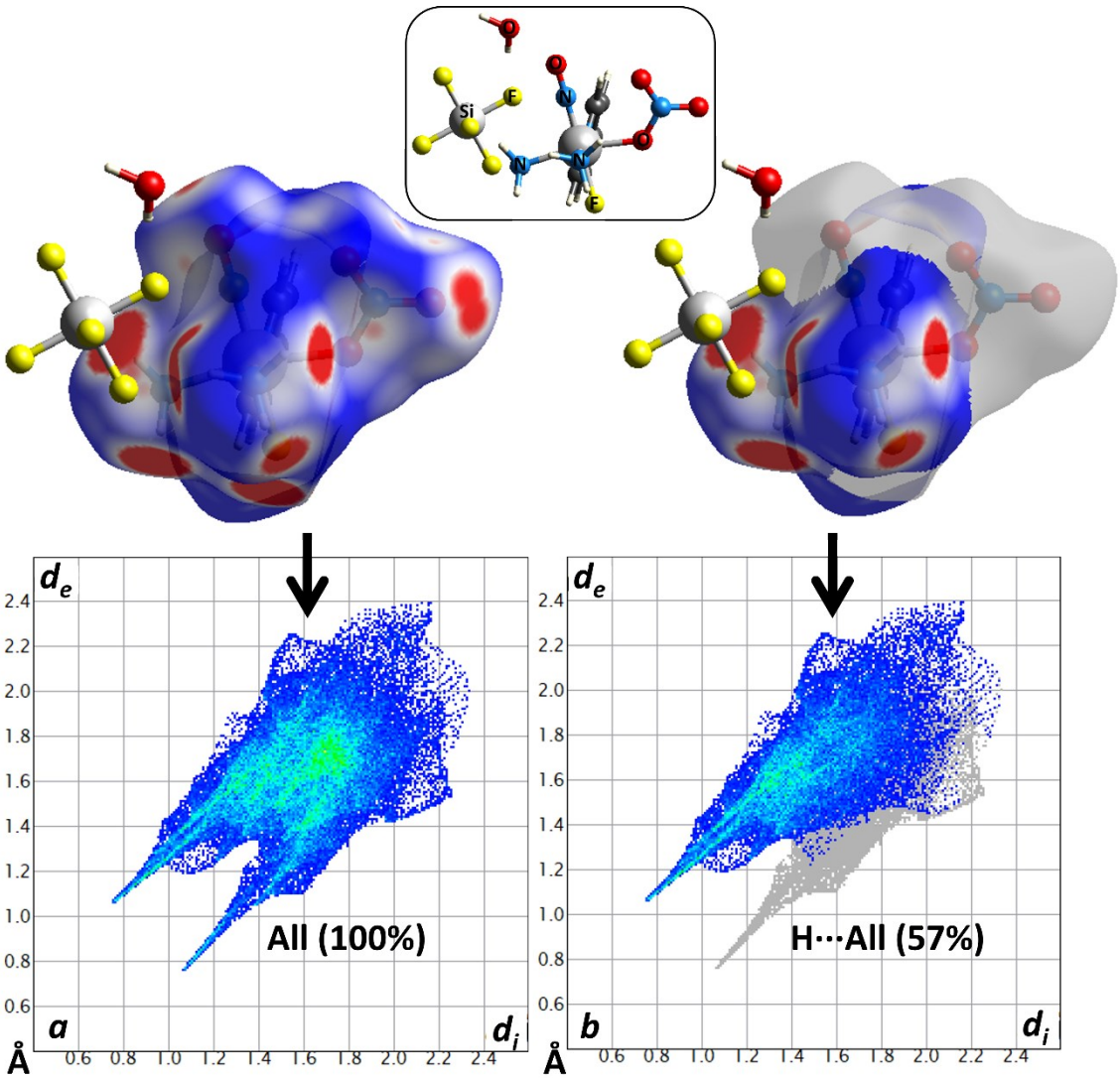

Fig. S4. The panel *a* represents the total Hirshfeld surface of the $[RuNO(NH_3)_2Py(NO_3)F]^+$ cation and corresponding two-dimensional fingerprint. The panel *b* shows the surface formed by the contacts of hydrogen atoms with other surrounding atoms and corresponding 2D fingerplot.

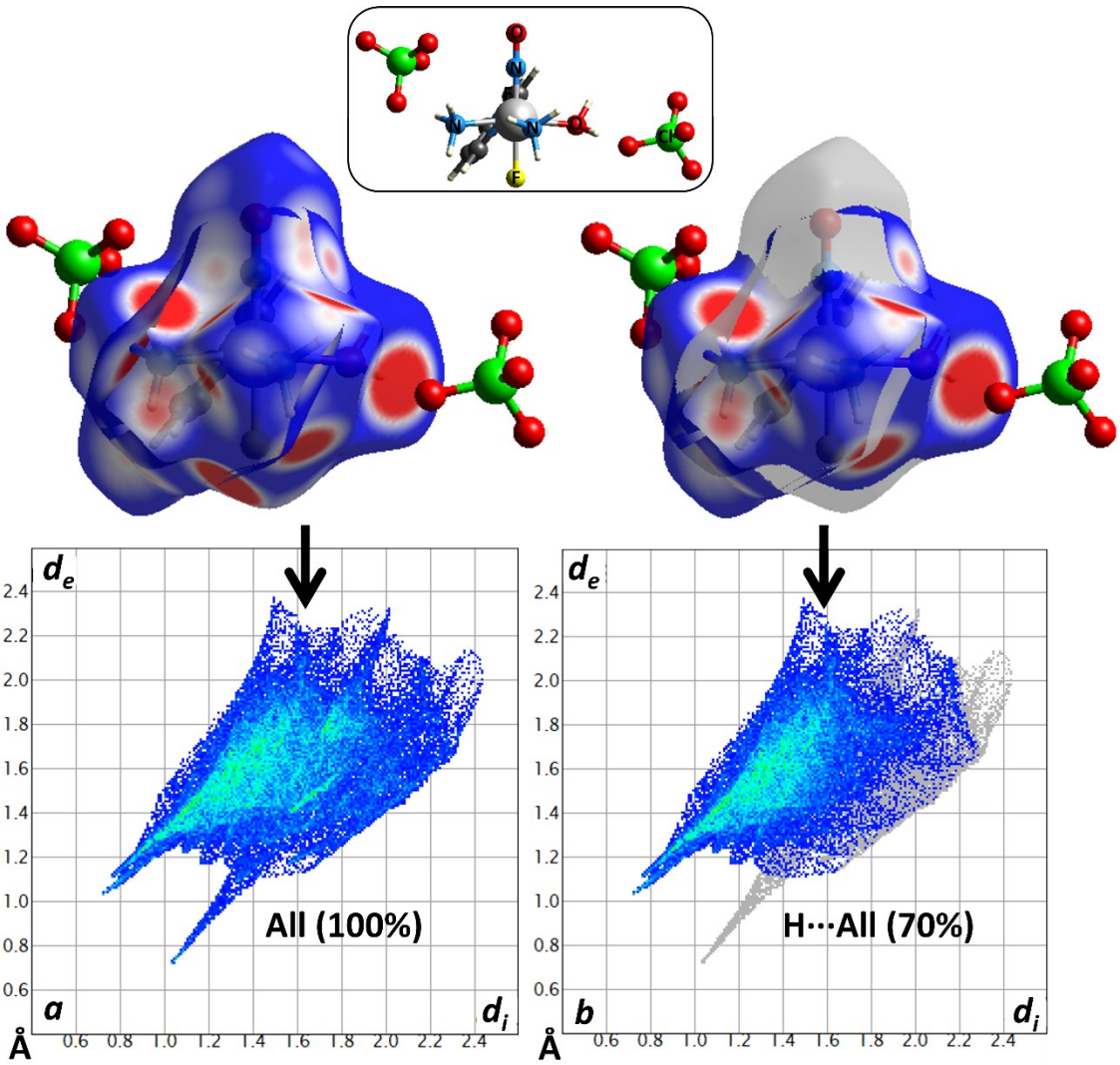

Fig. S5. The panel *a* represents the total Hirshfeld surface of the $[RuNO(NH_3)_2Py(H_2O)F]^{2+}$ cation and corresponding two-dimensional fingerprint. The panel *b* shows the surface formed by the contacts of hydrogen atoms with other surrounding atoms and corresponding 2D fingerplot.

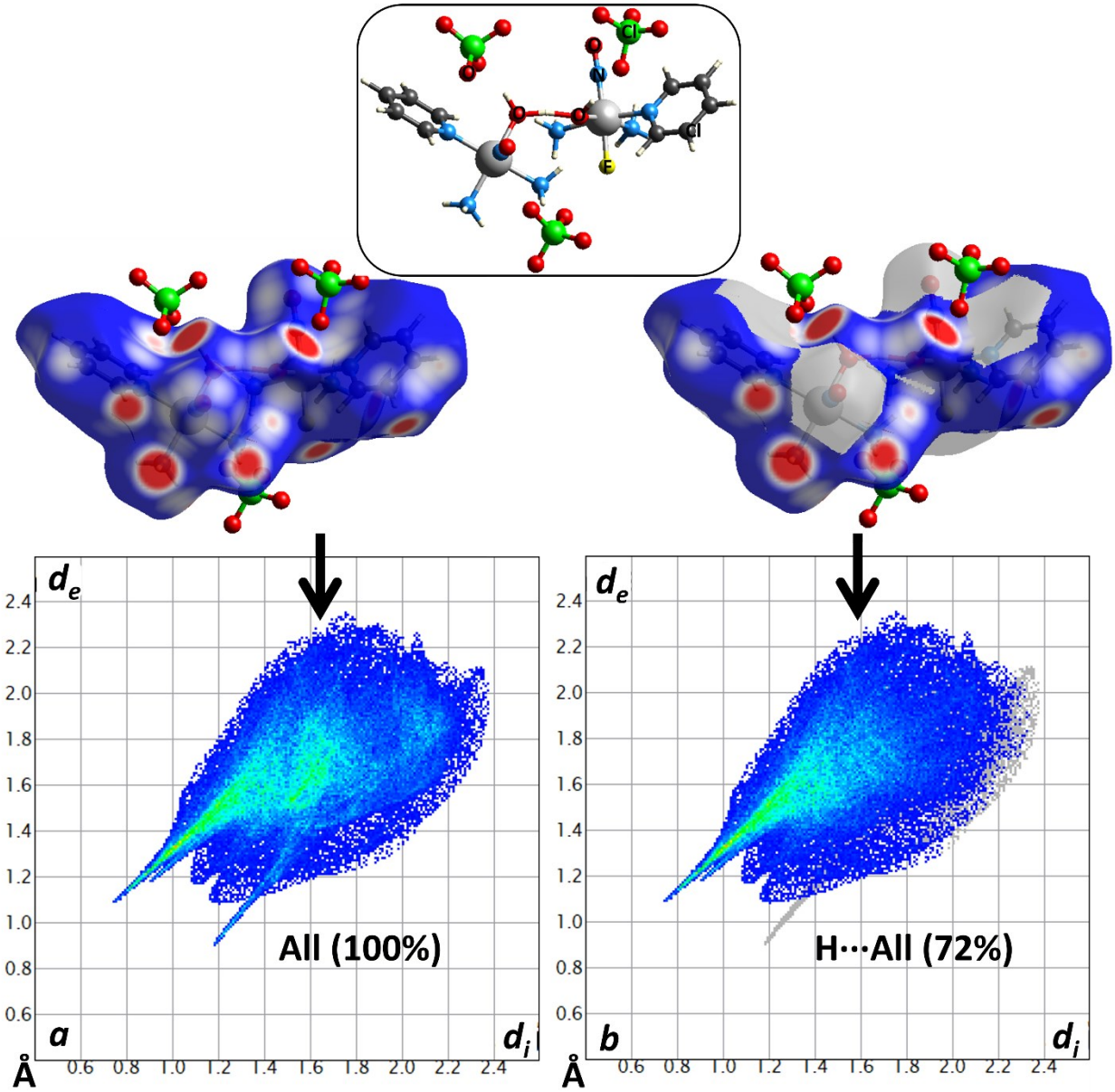

Fig. S6. The panel *a* represents the total Hirshfeld surface of the $[(RuNOPy(NH_3)_2F)_2(\mu\text{-}O_2H_3)]^{3+}$ cation and corresponding two-dimensional fingerprint. The panel *b* shows the surface formed by the contacts of hydrogen atoms with other surrounding atoms and corresponding 2D fingerplot.

Table S2. Intermolecular contacts of NO shorter than the sum of the van der Waals radii (contacting atoms are underlined).

I		II		III	
N<u>O</u>···F	2.85	N<u>O</u>···F	2.95	N<u>O</u>···O	2.97
N<u>O</u>···F	2.85	N<u>O</u>···O	2.84	<u>N</u>O···O	3.00
<u>N</u>O···F	2.87	N<u>O</u>···O	2.97	<u>N</u>O···O	3.01
<u>N</u>O···F	2.87	N<u>O</u>···C	3.10		
		N<u>O</u>···C	3.11		
		<u>N</u>O···O	2.87		

Table S3. The positions of ν(NO) bands of GS, MS1 and MS2; populations of MS1 and MS2; decay temperatures (T_d) of MS1 and MS2 in the different complexes with *trans*-ON-Ru-F coordinate.

	$\nu(NO)_{GS}$, cm^{-1}	$\nu(NO)_{MS1}$, cm^{-1}	$\nu(NO)_{MS2}$, cm^{-1}	MS1, %	MS2, %	T_d(MS1), K	T_d(MS2), K	Ref.
$[RuNO(NH_3)_2(H_2O)_2F]SiF_6$	1914	1778	1565	7	1	284	214	Present
$[RuNO(Py)_4F](ClO_4)_2$	1900	1762	1565	40	10	289	185	[3,4]
$[RuNO(NH_3)_2Py(H_2O)F](ClO_4)_2$	1923	1784	1564	26	6	290	213	Present
$[RuNO(NH_3)_4F](SiF_6)$	1902	1769	1545	10	3	292	206	[5]
$[RuNO(NH_3)_2Py(NO_3)F]_2SiF_6{\cdot}H_2O$	1933	1801	1587	12	5	294	194	Present
$[RuNO(NH_3)_4F](ClO_4)_2$	1874	1747	1494	7	1	303	-	[6]
$[RuNO(NH_3)_4F][PdCl_4]$	1896	1755	-	1	-	307	-	[6]

References

(1) Hirshfeld, F. L. Bonded-Atom Fragments for Describing Molecular Charge Densities. *Theor. Chim. Acta* **1977**, *44* (2), 129–138. https://doi.org/10.1007/BF00549096.

(2) Spackman, M. A.; Jayatilaka, D. Hirshfeld Surface Analysis. *CrystEngComm* **2009**, *11* (1), 19–32. https://doi.org/10.1039/B818330A.

(3) Kostin, G. A.; Mikhailov, A. A.; Kuratieva, N. V; Pishchur, D. P.; Makhinya, A. N. High Thermal Stability of the Ru–ON (MS1) Linkage Isomer of the Ruthenium Nitrosyl Complex [RuNO(Py) 4 F](ClO 4) 2 with the Trans NO–Ru–F Coordinate. *New J. Chem.* **2018**, *42* (23), 18928–18934. https://doi.org/10.1039/C8NJ04620D.

(4) Mikhailov, A. A.; Wenger, E.; Kostin, G. A.; Schaniel, D. Room-Temperature Photogeneration of Nitrosyl Linkage Isomers in Ruthenium Nitrosyl Complexes. *Chem. – A Eur. J.* **2019**, *25* (31), 7569–7574. https://doi.org/10.1002/chem.201901205.

(5) Mikhailov, A.; Vuković, V.; Kijatkin, C.; Wenger, E.; Imlau, M.; Woike, T.; Kostin, G.; Schaniel, D. Combining Photoinduced Linkage Isomerism and Nonlinear Optical Properties in Ruthenium Nitro-syl Complexes. *Acta Crystallogr. Sect. B Struct. Sci. Cryst. Eng. Mater.* **2019**, *75* (6), 1152–1163. https://doi.org/10.1107/S205252061901357X.

(6) Mikhailov, A. A.; Komarov, V. Y.; Sukhikh, A. S.; Pishchur, D. P.; Schaniel, D.; Kostin, G. A. The Impact of Counterion on the Metastable State Properties of Nitrosyl Ruthenium Complexes. *New J. Chem.* **2020**, *44* (41), 18014–18024. https://doi.org/10.1039/D0NJ04436A.